Lab - Mechatronics
Modelling and control of a Magnetic Levitation System

Tommaso Bocchietti 10740309
Daniele Cianca 10764733
Sara Orazzo 10995845

A.Y. 2024/25

POLITECNICO
MILANO 1863

Contents

List of Figures

List of Tables

Listings

1 Introduction

The aim of this laboratory experience is to precisely control the levitation of a ferromagnetic object immerse in a magnetic field. This kind of system is commonly referred to as a Magnetic Levitation System (MLS).
The work has been splitted into two main phases:

- **Modelling and parameters identification**: in this phase, the system has been modelled by means of both differential equations and state space representation, and the parameters of the model have been identified through experimental data performed directly on the real system. Some preliminary consideration about stability and controllability have also been made.
- **Control design**: in this phase, many different control techniques have been implemented and tested. The main goal was to compare the performances of different controllers in terms of stability, robustness and tracking capabilities.

Report structure This report covers all the aspects of the laboratory experience, from the theoretical background to the practical implementation of the control algorithms. In particular, in Section 2 a brief introduction to the MLS is given, along with some considerations about the physical phenomena involved. In Section 3 the model of the system is derived and some considerations about stability and controllability are made, while in Section 4 the parameters of the model are identified through experimental data or collected from the datasheet of the components. In Section 5 some estimators and filters are designed to reduce noise and improve the performances of the controllers designed in Section 6. Finally, in Section 7 some conclusions about the work done and possible future developments are drawn.

Tools An extensive use of `MATLAB` and `Simulink` has been made to implement the controllers and to simulate the system. All the source code and simulations used for this report can be found on the GitHub repository at the following link: `https://github.com/Bocchio01/062020-Lab-Mechatronics`.

2 Magnetic Levitation System

As stated in the introduction, the system under study is the Magnetic Levitation System (MLS) provided by `Inteco` (producer website: `https://www.inteco.com.pl/products/magnetic-levitation-systems/`). In Figure 1 the system used in this work is shown.

Figure 1: Magnetic Levitation System

As it can be seen quite clearly, the system is composed of a simple mechanical structure that is used to support two electromagnets and an optical infrared sensor. Along with the mechanical structure, a ferromagnetic ball and a control unit are present.
At its core principle, the system uses the interaction between the magnetic field generated by the electromagnets and the ferromagnetic ball to keep the ball in a desired position. The optical sensor is used to measure the position of the ball and provide feedback to the control unit that, in turn, adjusts the voltage applied to (and indeed the current flowing through) the electromagnets to keep the ball in a desired position. In Figure 2 a schematic representation of the upper half of the system is shown.

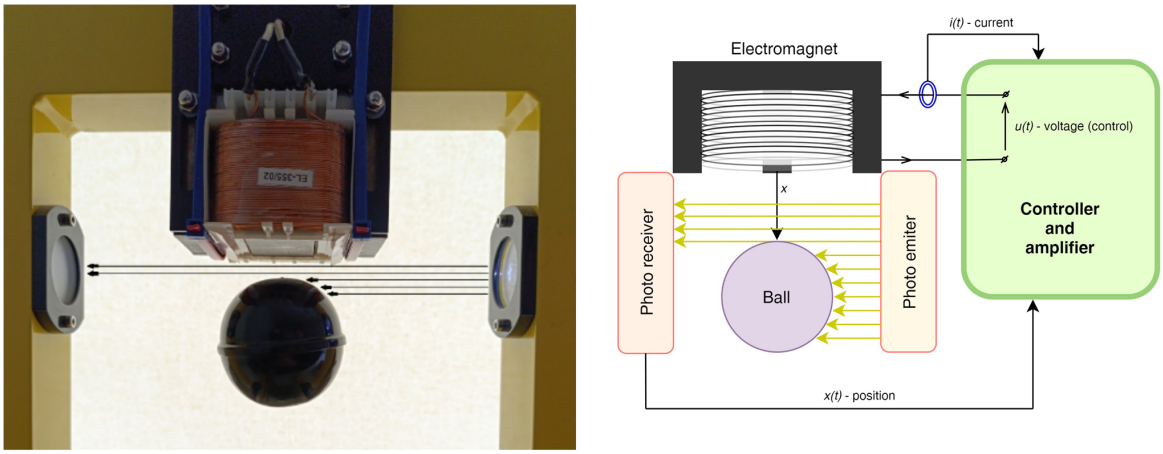

Figure 2: Schematic representation of the upper half of the MLS system.

Real world application Despite the fact that our system is a simplified use case, the magnetic levitation principle is used in many real-world applications.
One of the most common applications is the magnetic levitation trains, also known as 'MagLev' trains. These trains use the magnetic levitation principle to lift the train off the tracks and propel it forward using the magnetic

field generated by the tracks. The main advantage of this technology is the absence of friction between the train and the tracks, which allows the train to reach higher speeds and reduce the noise characteristic of the traditional trains. Some of the fastest (operating) trains in the world are MagLev trains, with the Shanghai MagLev train being the fastest, reaching a top speed of $623 km/h$ [1].
Another application of the magnetic levitation principle is the magnetic bearings. These bearings use the magnetic field generated by electromagnets to levitate a rotor and keep it in a desired position. The main advantage of this technology is the absence of mechanical contact between the rotor and the stator, which allows the rotor to reach higher speeds and reduce the wear of the components.

3 Modelling

The MLS is a complex system that can be divided into two main subsystems:

- **Electromagnetic subsystem**: it takes into account the electrical components of the system from the power supply to the generation of the magnetic field by the coils;
- **Mechanical subsystem**: it takes into account the dynamics of the ball and all the forces acting on it, including the electromagnetic forces generated by the magnetic field.

Due to the presence of the ball that moves inside a magnetic field, a complex connection between the two subsystems that goes beyond the simple force balance exists. For this reason, it's almost impossible to derive a complete model without considering both subsystems at the same time.
In Figure 3, a schematic representation of all the components and forces acting on the system is shown. Instead, in Table 3 a brief description of the components of the system and their units is reported.

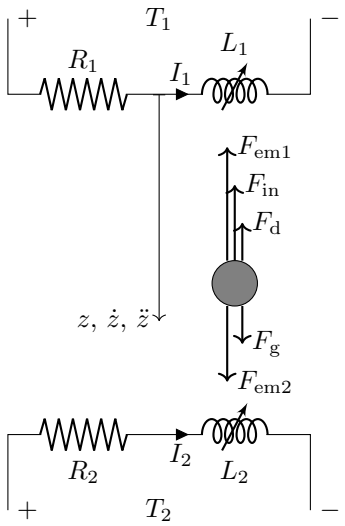

Name	Description	Units
F_g	Gravitational force	N
F_{in}	Inertial force	N
F_d	Drag force	N
$F_{em1,2}$	Electromagnetic force	N
$R_{1,2}$	Resistance of the coil	Ω
$L_{1,2}$	Inductance of the coil	H
$I_{1,2}$	Current flowing through the coil	A
$V_{1,2}$	Voltage applied to the coil	V
$T_{1,2}$	Temperature of the coil	$°C$

Figure 3: Schematic representation of the MLS system and description of the components.

In the following sections, we will derive the equations that governs the MLS system, adopting an energetic approach that starts from the energy conservation principle.

3.1 Mathematical model

We can now proceed with the derivation of the equations that govern the system.
At first, we can recall that the energy conservation principle states that the sum of the kinetic, potential, and dissipated energy of the system is equivalent to the work done by the external forces acting on the system.

3.1.1 Lagrange's equation

Thanks to the Lagrange's equation we write the following, that encaptulates the energy conservation principle:

$$\frac{d}{dt}\left(\frac{\partial \mathcal{T}}{\partial \dot{\mathbf{u}}}\right) - \frac{\partial \mathcal{T}}{\partial \mathbf{u}} + \frac{\partial \mathcal{D}}{\partial \dot{\mathbf{u}}} + \frac{\partial \mathcal{U}}{\partial \mathbf{u}} = \mathcal{Q} \tag{1}$$

Where $\mathbf{u}$ is the generalized coordinates of the system, $\mathbf{T}$ is the kinetic energy of the system, $\mathbf{D}$ is the dissipated energy of the system, $\mathbf{U}$ is the potential energy of the system, and $\mathbf{Q}$ is the generalized input to the system.
At first, we can give a definition of all the energetic terms included in Equation 1 for the MLS system. Notice that with respect to traditional purely mechanical systems, we also have to consider the stored energy in the coils as inductors, the dissipation due to the resistance of the coils, and the potential energy given by the external power supply.
By doing so, we can write the kinetic energy of the system as:

$$\mathcal{T} = \frac{1}{2}m\dot{z}^2 + \frac{1}{2}L_1(z, \dot{q_1}, T_1)\dot{q_1}^2 + \frac{1}{2}L_2(z, \dot{q_2}, T_2)\dot{q_2}^2 \tag{2}$$

Where m is the mass of the ball, L_1 and L_2 are the inductances of the coils, and q_1 and q_2 are the charges stored in the coils. It follows that $\dot{q_1}$ and $\dot{q_2}$ are the currents flowing through the coils.
The dissipated energy of the system can be written as:

$$\mathcal{D} = \int_{\dot{z}(\cdot)} \frac{1}{2} C_d A \rho \dot{z}^2 d\dot{z} + \int_{\dot{q_1}(\cdot)} R_1(\dot{q_1}, T_1) \dot{q_1} d\dot{q_1} + \int_{\dot{q_2}(\cdot)} R_2(\dot{q_2}, T_2) \dot{q_2} d\dot{q_2} \tag{3}$$

Where C_d is the drag coefficient, A is the cross-sectional area of the ball, and ρ is the density of the air.
Instead, the potential energy of the system can be written as:

$$\mathcal{U} = -mgz - q_1 V_1 - q_2 V_2 \tag{4}$$

Where V_1 and V_2 are the voltages applied to the coils.
Finally, the generalized input to the system can be evaluated as:

$$\mathcal{Q} = 0 \tag{5}$$

For convenience, we have chosen to consider both the external power supplied to the coils and the gravitational force as potential energy terms and not as generalized inputs. Notice also the minus sign in the gravitational potential energy term, which is due to the fact that the gravitational force increases the potential energy with respect to the chosen reference frame (positive downwards).

3.1.2 Electrical components model

Before proceeding, it's necessary to explicitly state the dependence of the inductance and resistance terms on the generalized coordinates of the system.
We can assume that, in first approximation, the sensitivity of both the electrical components to the temperature of the coils is negligible. This is strong and possibly incorrect assumption, but it allows us to simplify the model and focus on the main dynamics of the system.
For what regards the resistance terms, we can assume that the resistance of the coils is constant and so does not depend on neither the current flowing through them nor the temperature of the coils. For the assumption stated above, we can write the resistance terms as:

$$\begin{aligned} R_1 &= R_1(\dot{q_1}, T_1) = R_{10} \\ R_2 &= R_2(\dot{q_2}, T_2) = R_{20} \end{aligned} \tag{6}$$

Where R_{*0} are the resistances of the coils at ambient temperature with negligible current flowing through them.
Instead, considering the inductance terms, we will neglect the dependence on the coil's temperature, but we will take into account the variation of the inductance due to the presence of the ball in the magnetic field (principal source of nonlinearity in the system) and also the dependence over the current flowing through the coils. For the assumption stated above, we will try to model the inductance terms as:

$$\begin{aligned} L_1 &= L_1(z, \dot{q_1}, T_1) = L_{10} + L_{1z} e^{-a_1 z} + L_{1I} * \tanh(-b_1 * I_1) \\ L_2 &= L_2(z, \dot{q_2}, T_2) = L_{20} + L_{2z} e^{-a_2 (h-2r-z)} + L_{2I} * \tanh(-b_2 * I_2) \end{aligned} \tag{7}$$

Where L_{*0} are the nominal inductances values. Instead, L_{*z}, a_* and L_{*I}, b_* are coefficients that take into account the variation of the inductance due to the presence of the ball in the magnetic field and the current flowing through the coils, respectively.
It has to be noted that this model was suggested by a careful analysis of experimental data and is not directly based on theoretical considerations. Some previous models of inductance can also be found in the literature, but they are often too complex and not suitable for control purposes.

3.1.3 Equations of motion

To derive the equations of motion of the system, we can substitute the kinetic (2), dissipated (3), and potential energy (4) terms into the Lagrange's equation (1). By a qualitative analysis of the system, recalling also that we have chosen to neglect the effect of coil's temperature for the electrical components, we can see that the generalized coordinates are z, q_1, and q_2, and so the vector of generalized coordinates is $\mathbf{u} = [z, q_1, q_2]^T$.
Once $\mathbf{u}$ has been identified, the procedure to derive the equations of motion is straightforward. Following Equation 1, we can write the following system of equations:

$$\begin{cases} \frac{d}{dt}\left(\frac{\partial \mathcal{T}}{\partial \dot{z}}\right) - \frac{\partial \mathcal{T}}{\partial z} + \frac{\partial \mathcal{D}}{\partial \dot{z}} + \frac{\partial \mathcal{U}}{\partial z} = \mathcal{Q} \\ \frac{d}{dt}\left(\frac{\partial \mathcal{T}}{\partial \dot{q_1}}\right) - \frac{\partial \mathcal{T}}{\partial q_1} + \frac{\partial \mathcal{D}}{\partial \dot{q_1}} + \frac{\partial \mathcal{U}}{\partial q_1} = \mathcal{Q} \\ \frac{d}{dt}\left(\frac{\partial \mathcal{T}}{\partial \dot{q_2}}\right) - \frac{\partial \mathcal{T}}{\partial q_2} + \frac{\partial \mathcal{D}}{\partial \dot{q_2}} + \frac{\partial \mathcal{U}}{\partial q_2} = \mathcal{Q} \end{cases} \tag{8}$$

By substituting the energetic terms obtained in Equations 2, 3, 4, 5 into the set of equations above, we obtain the following equations of motion:

$$\begin{cases} m\ddot{z} - \frac{1}{2}\frac{\partial L_1}{\partial z}\dot{q_1}^2 - \frac{1}{2}\frac{\partial L_2}{\partial z}\dot{q_2}^2 + \frac{1}{2}C_d A\rho\dot{z}|\dot{z}| - mg = 0 \\ \frac{1}{2}\left(\frac{\partial^2 L_1}{\partial \dot{q_1}\partial z}\dot{z} + \frac{\partial^2 L_1}{\partial \dot{q_1}^2}\ddot{q_1}\right)\dot{q_1}^2 + \frac{\partial L_1}{\partial \dot{q_1}}\dot{q_1}\ddot{q_1} + \left(\frac{\partial L_1}{\partial z}\dot{z} + \frac{\partial L_1}{\partial \dot{q_1}}\ddot{q_1}\right)\dot{q_1} + L_1\ddot{q_1} + R_1\dot{q_1} - V_1 = 0 \\ \frac{1}{2}\left(\frac{\partial^2 L_2}{\partial \dot{q_2}\partial z}\dot{z} + \frac{\partial^2 L_2}{\partial \dot{q_2}^2}\ddot{q_2}\right)\dot{q_2}^2 + \frac{\partial L_2}{\partial \dot{q_2}}\dot{q_2}\ddot{q_2} + \left(\frac{\partial L_2}{\partial z}\dot{z} + \frac{\partial L_2}{\partial \dot{q_2}}\ddot{q_2}\right)\dot{q_2} + L_2\ddot{q_2} + R_2\dot{q_2} - V_2 = 0 \end{cases} \tag{9}$$

For convenience, we can replace time derivatives of charges with currents by using the definition of current as the time derivative of the charge. Moreover, we can group the terms in the equations above so to move higher order derivatives to the left-hand side of the equations. Finally, we also transform the second order differential equations into first order differential equations by introducing a fourth equation and considering the ball velocity v as a state variable. By doing so, we obtain the following set of equations:

$$\begin{cases} \dot{z} = v \\ \dot{v} = m^{-1}\left(\frac{1}{2}\frac{\partial L_1}{\partial z}I_1^2 + \frac{1}{2}\frac{\partial L_2}{\partial z}I_2^2 - \frac{1}{2}C_d A\rho\dot{z}|\dot{z}| + mg\right) \\ \dot{I_1} = \left(\frac{1}{2}\frac{\partial^2 L_1}{\partial I_1^2}I_1^2 + 2\frac{\partial L_1}{\partial I_1}I_1 + L_1\right)^{-1}\left(-\frac{1}{2}\frac{\partial^2 L_1}{\partial I_1 \partial z}\dot{z}I_1^2 - \frac{\partial L_1}{\partial z}\dot{z}I_1 - R_1 I_1 + V_1\right) = 0 \\ \dot{I_2} = \left(\frac{1}{2}\frac{\partial^2 L_2}{\partial I_2^2}I_2^2 + 2\frac{\partial L_2}{\partial I_2}I_2 + L_2\right)^{-1}\left(-\frac{1}{2}\frac{\partial^2 L_2}{\partial I_2 \partial z}\dot{z}I_2^2 - \frac{\partial L_2}{\partial z}\dot{z}I_2 - R_2 I_2 + V_2\right) = 0 \end{cases} \tag{10}$$

The set of equations above represents the complete mathematical model of the MLS system. One can notice that the equations are both nonlinear and coupled, making the system hard to analyze and control.

3.1.4 Model reduction

In order to simplify the model and make it more suitable for control purposes, we can make some assumptions that allow us to reduce the complexity of the system.
Based also on the experimental data collected during the parameters identification phase (Section **??**), we can state that the sensitivity of the inductance terms to the current flowing through the coils is negligible around the operating point. Moreover, also the velocity of the ball will always be small, and so every term that is linearly dependent on it can be neglected. By doing so, we can impose the following conditions to the system:

$$\begin{cases} \frac{\partial L_*}{\partial I_*} & \approx 0 \\ \frac{\partial^2 L_*}{\partial I_*^2} & \approx 0 \\ \dot{z} & \approx 0 \end{cases} \tag{11}$$

By doing so, we can simplify the equations of motion as:

$$\begin{cases} \dot{z} = v \\ \dot{v} = m^{-1}\left(\frac{1}{2}\frac{\partial L_1}{\partial z}I_1^2 + \frac{1}{2}\frac{\partial L_2}{\partial z}I_2^2 + mg\right) \\ \dot{I_1} = L_1^{-1}\left(-R_1 I_1 + V_1\right) \\ \dot{I_2} = L_2^{-1}\left(-R_2 I_2 + V_2\right) \end{cases} \tag{12}$$

3.1.5 Control input adaptation

A final important remark has to be made about the so-called *black zone* of the system, that are the regions where the current flowing through the coils is no more reachable.
In particular, by simply connect the power supply to the coils, a minimum voltage will be applied and a certain amount of current will flow through the coils. In the following, we will refer to this current and voltage as I_{*min} and V_{*min} respectively.
Because of this, the above derived model must be slightly modified to take into account the black zone of the system.
In particular, the set of Equations 12 can be rewritten as:

$$\begin{cases} \dot{z} = v \\ \dot{v} = m^{-1}\left(\frac{1}{2}\frac{\partial L_1}{\partial z}I_1^2 + \frac{1}{2}\frac{\partial L_2}{\partial z}I_2^2 + mg\right) \\ \dot{I_1} = L_1^{-1}\left(-R_1 I_1 + (k_1 U_1 + c_1)\right) \\ \dot{I_2} = L_2^{-1}\left(-R_2 I_2 + (k_2 U_2 + c_2)\right) \end{cases} \tag{13}$$

3.2 Model Linearization

The model derived in the previous subsection is highly non-linear. In order to begin able to apply linear control techniques, it is necessary to linearize the model around a given operating point.

3.2.1 Operating Point Computation

The operating point is the set of values of the state and input variables around which the linearization is performed.
Given the set of Equations 13, the operating point can be computed by setting the time derivatives to zero, set at least 2 of the state variables or input variables to constant values and solve the system of equations. Based on the physical meaning of the state and input variables, it's reasonable to set the position of the ball z and the current in the lower electromagnet I_2 to constant values. By doing so, all the other state and input variables can be computed by solving the following set of equations:

$$\mathbf{x}_{op} = \begin{bmatrix} z_{op} \\ v_{op} \\ I_{1op} \\ I_{2op} \end{bmatrix} = \begin{cases} z_{star} \\ 0 \\ \sqrt{-(2mg + \frac{\partial L_2}{\partial z} I_{2op}^2)/\frac{\partial L_1}{\partial z}} \\ I_{2star} \end{cases} \tag{14}$$

$$\mathbf{u}_{op} = \begin{bmatrix} U_{1op} \\ U_{2op} \end{bmatrix} = \begin{cases} \max\left[0, R_{10}\left(I_{1op} - I_{1min}\right)/k_1\right] \\ \max\left[0, R_{20}\left(I_{2op} - I_{2min}\right)/k_2\right] \end{cases} \tag{15}$$

Where z_{star} is the desired position of the ball and I_{2star} is the desired current in the lower electromagnet. As we can see, once those values are set, all the other states and inputs can be computed uniquely.

3.2.2 Linearized Model Derivation

Based on the operating point computed in the previous subsection, the linearized model can be obtained by performing a Taylor expansion around the operating point up to the first order terms of Equations 13 or Equations 33.
Before performing the linearization, we briefly recall the general form of a Taylor expansion of a function $f(\mathbf{x})$ around a point $\mathbf{x}_{op}$:

$$f(\mathbf{x}) \approx f(\mathbf{x}_{op}) + \nabla f(\mathbf{x}_{op}) \cdot (\mathbf{x} - \mathbf{x}_{op}) \tag{16}$$

Where $\nabla f(\mathbf{x}_{op})$ is the gradient of $f(\mathbf{x})$ evaluated at $\mathbf{x}_{op}$.
By applying the Taylor expansion to the non-linear model, the linearized model can be obtained as:

$$\mathbf{f}(\mathbf{x}) - \mathbf{f}(\mathbf{x}_{op}) \approx \left.\frac{\partial \mathbf{f}}{\partial \mathbf{x}}\right|_{\mathbf{x}_{op}} \cdot (\mathbf{x} - \mathbf{x}_{op}) \tag{17}$$

Considering now the set of Equations 13, the linearized model can be obtained as:

$$\begin{cases} \dot{z} - \dot{z_{op}} & \approx 1(v - v_{op}) \\ \dot{v} - \dot{v_{op}} & \approx m^{-1}\left(\left.\frac{1}{2}\frac{\partial^2 L_1}{\partial z^2}\right|_{\mathbf{x}_{op}} (z - z_{op}) I_{1op}^2 + \left.\frac{1}{2}\frac{\partial^2 L_2}{\partial z^2}\right|_{\mathbf{x}_{op}} (z - z_{op}) I_{2op}^2 + \left.\frac{\partial L_1}{\partial z}\right|_{\mathbf{x}_{op}} I_{1op}(I_1 - I_{1op}) + \left.\frac{\partial L_2}{\partial z}\right|_{\mathbf{x}_{op}} I_{2op}(I_2 - I_{2op})\right) \\ \dot{I}_1 - \dot{I_{1op}} & \approx \left(-L_1^{-2}\frac{\partial L_1}{\partial z}\left(-R_1 I_1 + k_1 U_1 + c_1\right)\right)\Big|_{\mathbf{x}_{op}} (z - z_{op}) + \left(-L_1^{-1} R_1\right)\Big|_{\mathbf{x}_{op}} (I_1 - I_{1op}) + \left(L_1^{-1} k_1\right)\Big|_{\mathbf{x}_{op}} (U_1 - U_{1op}) \\ \dot{I}_2 - \dot{I_{2op}} & \approx \left(-L_2^{-2}\frac{\partial L_2}{\partial z}\left(-R_2 I_2 + k_2 U_2 + c_2\right)\right)\Big|_{\mathbf{x}_{op}} (z - z_{op}) + \left(-L_2^{-1} R_2\right)\Big|_{\mathbf{x}_{op}} (I_2 - I_{2op}) + \left(L_2^{-1} k_2\right)\Big|_{\mathbf{x}_{op}} (U_2 - U_{2op}) \end{cases} \tag{18}$$

Notice that in the derivation of the linearized model, another model reduction has been performed based on the same assumptions made in the previous subsection with the set of Equations 11.

3.3 State Space Representation

In the optics of control theory, it is useful to represent the system in the state space form. The state space representation is a mathematical model of a physical system as a set of input, output and state variables related by first-order differential equations. The state space representation is particularly useful for linear systems, as it allows to easily apply linear control techniques.
A generic nonlinear system can be represented in the state space form as:

$$\begin{aligned} \dot{\mathbf{x}} &= f(\mathbf{x}, \mathbf{u}) \\ \mathbf{y} &= g(\mathbf{x}, \mathbf{u}) \end{aligned} \tag{19}$$

Where $\mathbf{x}$ is the state vector and $\mathbf{u}$ is the input vector.
Similarly to what has been done in the previous subsection, we can perform a linearization of the system around an operating point to obtain the linearized state space representation in the form of:

$$\begin{aligned} \dot{\delta\mathbf{x}} &\approx A\delta\mathbf{x} + B\delta\mathbf{u} \\ \delta\mathbf{y} &\approx C\delta\mathbf{x} + D\delta\mathbf{u} \end{aligned} \tag{20}$$

Where $\delta\mathbf{x}$ and $\delta\mathbf{u}$ are the deviations of the state and input vectors from the operating point, respectively. While the matrices A, B, C and D are the Jacobian matrices with respect to the state and input vectors evaluated at the operating point.

MagLev System State Space Representation Given the linearized model derived in the previous subsection, we can define the state vector $\mathbf{x}$ and the input vector $\mathbf{u}$ as:

$$\mathbf{x} = \begin{bmatrix} z \\ v \\ I_1 \\ I_2 \end{bmatrix} \quad \mathbf{u} = \begin{bmatrix} U_1 \\ U_2 \end{bmatrix} \tag{21}$$

Once the state and input vectors have been defined, the linearized state space representation can be obtained by leveraging the linearized model derived in the previous subsection. The matrices A, B, C and D are then defined as:

$$\begin{aligned} A &= \left.\frac{\partial f}{\partial \mathbf{x}}\right|_{(\mathbf{x}_{op}, \mathbf{u}_{op})} = \begin{bmatrix} 0 & 1 & 0 & 0 \\ a_{21} & 0 & a_{23} & a_{24} \\ a_{31} & 0 & a_{33} & 0 \\ a_{41} & 0 & 0 & a_{44} \end{bmatrix} \\ B &= \left.\frac{\partial f}{\partial \mathbf{u}}\right|_{(\mathbf{x}_{op}, \mathbf{u}_{op})} = \begin{bmatrix} 0 & 0 \\ 0 & 0 \\ b_{31} & 0 \\ 0 & b_{42} \end{bmatrix} \\ C &= \left.\frac{\partial g}{\partial \mathbf{x}}\right|_{(\mathbf{x}_{op}, \mathbf{u}_{op})} = \begin{bmatrix} 1 & 0 & 0 & 0 \end{bmatrix} \\ D &= \left.\frac{\partial g}{\partial \mathbf{u}}\right|_{(\mathbf{x}_{op}, \mathbf{u}_{op})} = \begin{bmatrix} 0 & 0 \end{bmatrix} \end{aligned} \tag{22}$$

By leveraging the linearization of the model derived in the previous subsection and reported in Equation 18, the elements of the matrices A, B, C and D can be computed as:

$$
\begin{aligned}
a_{21} &= \frac{1}{m}\left(\frac{1}{2}\frac{\partial^2 L_1}{\partial z^2}I_1^2 + \frac{1}{2}\frac{\partial^2 L_2}{\partial z^2}I_2^2\right)\Big|_{(\mathbf{x}_{op},\mathbf{u}_{op})} \\
a_{23} &= \frac{1}{m}\left(\frac{\partial L_1}{\partial z}I_1\right)\Big|_{(\mathbf{x}_{op},\mathbf{u}_{op})} \\
a_{24} &= \frac{1}{m}\left(\frac{\partial L_2}{\partial z}I_2\right)\Big|_{(\mathbf{x}_{op},\mathbf{u}_{op})} \\
a_{31} &= \left(-L_1^{-2}\frac{\partial L_1}{\partial z}\left(-R_1 I_1 + k_1 U_1 + c_1\right)\right)\Big|_{(\mathbf{x}_{op},\mathbf{u}_{op})} \\
a_{33} &= \left(L_1^{-1}(-R_1)\right)\big|_{(\mathbf{x}_{op},\mathbf{u}_{op})} \\
a_{41} &= \left(-L_2^{-2}\frac{\partial L_2}{\partial z}\left(-R_2 I_2 + k_2 U_2 + c_2\right)\right)\Big|_{(\mathbf{x}_{op},\mathbf{u}_{op})} \\
a_{44} &= \left(L_2^{-1}(-R_2)\right)\big|_{(\mathbf{x}_{op},\mathbf{u}_{op})} \\
b_{31} &= \left(L_1^{-1}k_1\right)\big|_{(\mathbf{x}_{op},\mathbf{u}_{op})} \\
b_{42} &= \left(L_2^{-1}k_2\right)\big|_{(\mathbf{x}_{op},\mathbf{u}_{op})}
\end{aligned}
\tag{23}
$$

4 Identification

In order to control the system, we need to identify its parameters.
To do so, different tests type will be performed, such as:

1. Direct measurement: measure all the quantity of the system that can be directly measured or retrieved from well established literature;
2. Sensors characterization: create the mapping between the position of the ball and the output voltage of the infrared sensor and study the variance of all the sensors used internally in the control unit;
3. Control to voltage: observe the relation between the control signal and the effective voltage applied to the coils;
4. Inductances characterization: identify all the parameters needed to characterize inductances, based on the model proposed in Equation 7;
5. Force validation: measure the force applied to the ball by the inductance in order to validate both the model and the parameters identified in the previous tests.

Except for the first test, all the others will be performed leveraging the data acquisition system included in the `Inteco` control unit.

4.1 Direct measurement

In this section, we will measure all the quantities that can be directly measured or retrieved from well established literature.
Most of the following parameters can be directly measured using a scale and a caliper, respectively. By doing so, we will have the following values:

Parameter	Value	Units
g	9.81	m/s^2
m	0.06157	kg
r	0.06125/2	m
H	0.098	m

Table 1: Directly measured parameters and constants

4.2 Sensors characterization

To be rewritten in a better form.
We need to create the mapping between the position of the ball and the output voltage of the infrared sensor. To do so, we simply create an array of points where we measure the position of the ball using a caliper and the output voltage of the infrared sensor using the data acquisition system included in the `Inteco` control unit.
The obtained data is shown in Figure 4.

Figure 4: Position to voltage identification

As we can see, the relation between the position of the ball and the output voltage of the infrared sensor can be approximated as linear outside the limits of the sensor.
From the data obtained, one can clearly see that for distances of the ball from the upper coil grater than $\approx 20[mm]$, the sensor reaches its saturation limit and the output voltage is constant. Based on this observation, we can also impose that during simulations, the maximum distance of the ball from the upper coil is $20[mm]$.
As a second step, we also need to study the variance of all the sensors used internally in the control unit. We now suppose for both the infrared sensor for position and the current sensor that their model is Gaussian. Based on this assumption, one can compute

4.3 Control to voltage

As said in the previous section of mathematical modeling, we need to identify the relation between the control signal and the effective voltage applied to the coils. The control unit provided by `Inteco` it's programmed to receive a PWM duty cycle as input and to convert it into a voltage that is applied to the coils. In order to identify this relation, we simply apply many duty cycles to the control unit and measure the corresponding voltage applied to the coils using a multimeter.
The output of this test is a series of points that can be fitted to a linear model having an initial black zone where the control action is not effective on the voltage applied to the coils. In Figure 5 we can observe both the measured points, the linear fitting and the effective voltage applied considering the black zone.

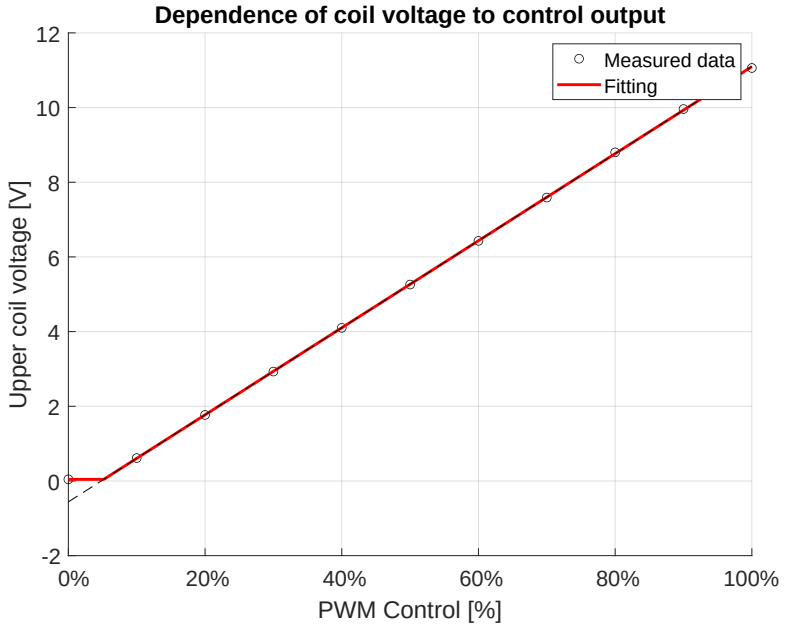

Figure 5: Control to voltage identification

As we can see, the linear model for the relation $V_* = f(U) = f(\text{PWM})$ is a good approximation outside the initial black zone control. Because of this, we can consider the following control to voltage relation:

$$V_* = \begin{cases} V_{*min} & \text{if } U < U_{min} \\ k_* U + c_* & \text{if } U \geq U_{min} \end{cases} \tag{24}$$

Where V_{*min} is the minimum voltage applied to the coils when the control signal is zero, u_{min} is the minimum control signal that is effective on the voltage applied to the coils, k_* is the slope of the linear model and c_* is the offset of the linear model.
The values of the parameters are shown in Table 2.

Parameter	Value	Units
V_{*min}	$4.300000 \cdot 10^{-2}$	V
U_{min}	5.179276	%
k_*	$1.165800 \cdot 10^{1}$	$V/\%$
c_*	$-5.608000 \cdot 10^{-1}$	V

Table 2: Control to voltage identification parameters

4.4 Inductances characterization

A key parameter of the system is the inductance of the coils.
As already proposed in Equation 7, the inductance of the coils cannot be considered constant and both its dependence on the current and the position of the ball must be taken into account when dealing with the magnetic levitation system.
In order to identify the inductance of the coils and all the parameters needed to characterize them, we have to measure the values of L_1 and L_2 for many currents and ball positions. Once we have these values, we can fit the data to the model proposed in Equation 7 and identify the parameters.

Given a certain (fix in time) position of the ball and a certain current step input, we can measure the value of the inductance of the coils, knowing that:

$$V = RI + \frac{d(LI)}{dt} = RI + \left(\frac{\partial L}{\partial I} I + L\right) \dot{I} \tag{25}$$

If we suppose for a moment that the variation of the inductance with the current is negligible, we can obtain a closed form solution for the current in the RL circuit as follows:

$$I(t) = \frac{V_{max}}{R_0} \left(1 - e^{-\frac{R_0}{L_0} t}\right) \tag{26}$$

Given the previous equation, we can adopt the following strategy to fully characterize the inductance of the coils over the range of possible ball positions and currents:

1. Fix the ball at a certain height (z^*);
2. Apply a certain current step input to the system (I^*);
3. Measure the current in the coils ($I(t)$);
4. Fit the measured current to the model proposed in Equation 26 and identify $L(z^*, I^*)$;
5. Repeat from step 2 for different step inputs of currents;
6. Repeat from step 1 for different ball positions.

In Figure 6 we can see on the left all the dynamics of the current in the coils for different step inputs of currents and different ball positions, while on the right we can see the fitting of the data to the model proposed in Equation 26.

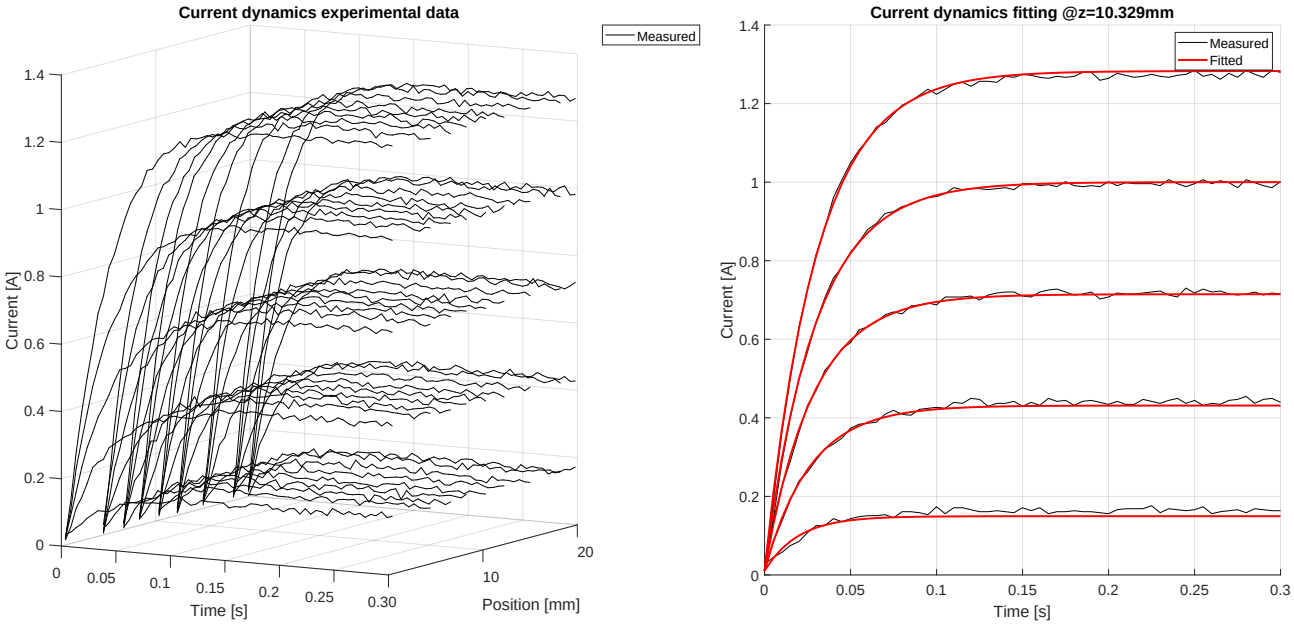

Figure 6: Inductance characterization for different currents and ball positions

From the right side of Figure 6 we can see that the fitting of the data to the model proposed in Equation 26 is optimal for middle values of the current, while it tends to underestimate and overestimate the current for low and high values of the current, respectively. This behavior is probably due to the fact that the variation of the inductance with the current that has been neglected in the model of the current (Equation 26) is not negligible and should have been taken into account.
Thanks to the data obtained from the multiple tests, we can now fit the values of the inductance of the coils to the model proposed in Equation 7 and identify the parameters. The obtained model fitting is shown in Figure 7.

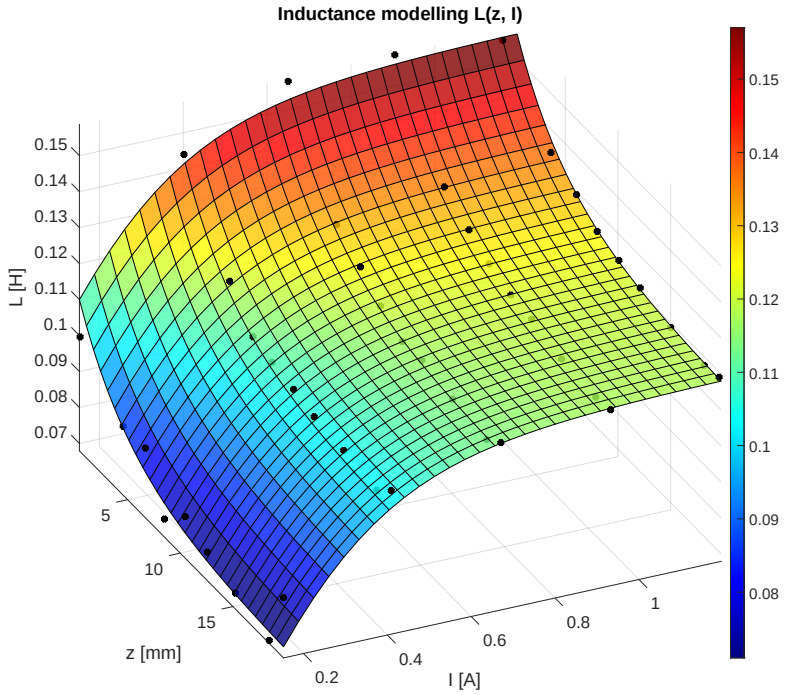

Figure 7: Inductance characterization

One can clearly see the 90 points that have been used to fit the model proposed in Equation 7 and the obtained fitting. The values of the parameters are shown in Table 3.

Parameter	Value	Units
L_0	$4.106763e-02$	H
a_z	$2.155909e+02$	$1/m$
L_z	$4.288065e-02$	H
a_I	$2.553122e+00$	$1/A$
L_I	$-7.675453e-02$	H

Table 3: Inductance characterization parameters

4.5 Force validation

The last test that we will perform is the force validation.
Thanks to the data obtained from the previous tests, we should already be able to predict the force applied to the ball by the inductance. In particular, we already know that the electromagnetic force applied to the ball is given by the following equation:

$$F_{em} = \frac{1}{2}\frac{\partial L}{\partial z} I^2 \tag{27}$$

Because of the previously identified parameters, we have an analytical expression for the sensitivity of the inductance with respect to the position of the ball. However, due to uncertainties in the identification of the parameters, we can expect some discrepancies between the predicted force and the measured one.
In order to quantify these discrepancies and validate the model, we will use a direct method to measure the force applied to the ball by the inductance and compare it with the predicted one. To do so, we recall Equation 13 and in particular the equation relative to $\dot{v}$:

$$\dot{v} = m^{-1}\left(\frac{1}{2}\frac{\partial L_1}{\partial z} I_1^2 + \frac{1}{2}\frac{\partial L_2}{\partial z} I_2^2 + mg\right) \tag{28}$$

If we consider the system at rest, we can simplify the equation as follows:

$$0 = \frac{1}{2}\frac{\partial L_1}{\partial z} I_1^2 + \frac{1}{2}\frac{\partial L_2}{\partial z} I_2^2 + mg \tag{29}$$

Supposing now that only the first coil is energized, we can further simplify the equation as follows:

$$0 = \frac{1}{2}\frac{\partial L_1}{\partial z} I_1^2 + mg \tag{30}$$

Which leads to:

$$\frac{\partial L_1}{\partial z} = -2\frac{mg}{I_1^2} \tag{31}$$

This last equation basically tells us that in steady state conditions, when the ball is levitating (i.e. $\dot{z} = 0$ and not supported by any platform), the sensitivity of the inductance of the first coil has an analytical expression that can be directly measured by measuring the current in the first coil.
In order to follow this approach, a linearly increasing voltage has been applied to the first coil and the current corresponding to the levitation of the ball has been measured. The test has been repeated for different initial positions of the ball, in order to fully characterize the dynamic inductance characteristics over the range of possible ball positions.
In Figure 8 we can see both the position of the ball and the current circulating in the first coil. By identifying the current at which the ball starts to levitate (i.e. the ball starts to move upwards), we can than use Equation 31 to identify the dynamic inductance characteristics.

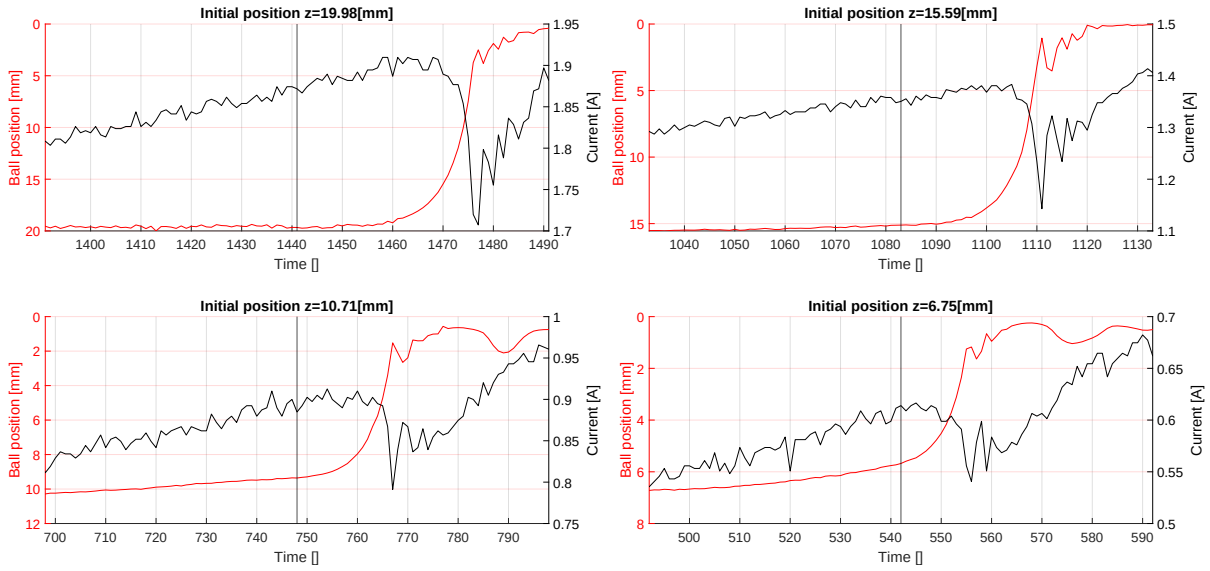

Figure 8: Position of the ball and current in the first coil around the levitation point (marked by vertical black line)

In Figure 9, we can observe both the measured data and the fitted ones. On the right side figure, a complete characterization of the electromagnetic force has been reconstructed based again on the above equations.

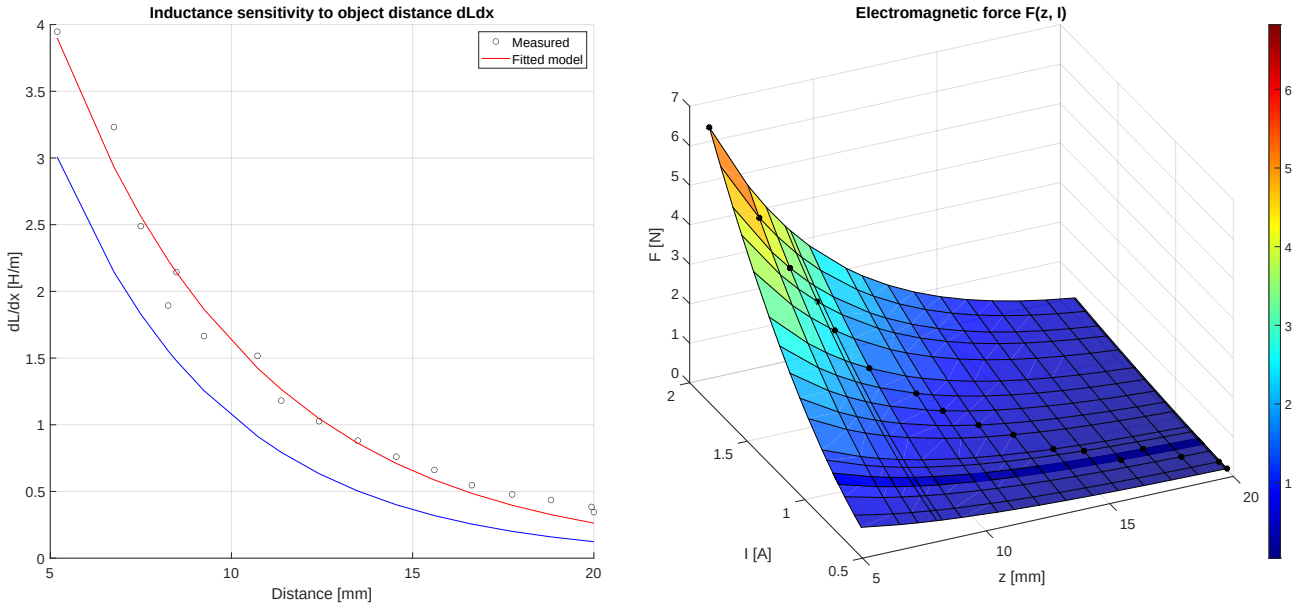

Figure 9: Dynamic inductance characteristics and electromagnet force

The left-hand side of Figure 9 shows a comparison between the measured data (black circles), their fitting (red line), the sensitivity of the inductance coming from the model (blue line) and the sensitivity of the inductance resulting from the literature parameters (green line). Notice that the curve coming from the literature parameters has been doubled given the different model used for the electromagnetic force in the literature (see Equation 33).
Data shows great accuracy in almost the entire range of the ball position, with a slight discrepancy in the lower part of the range. This discrepancy is probably due to poor measurement quality because of high noise ratio given by the infrared sensor.
The right-hand side of Figure 9 shows the electromagnetic force generated by the first coil as a function of both the ball position and the current circulating in the coil. One can notice that the force has an exponential behavior with respect to the ball position and a quadratic behavior with respect to the current.

5 Estimators & Filters Design

5.1 Low Pass Filter

5.2 Kalman Filter

5.3 Extended Kalman Filter

6 Controllers Design

In this section, we move on the design of the controllers that will be used to control the system.
As we have clarified in the previous section, the system is highly nonlinear with respect to both position and current, and we control it by acting on the input PWM signal.
In the following, we will present three main families of controllers that have been adopted for the control of the system: the Proportional-Integral-Derivative (PID) controller, the Linear Quadratic Regulator (LQR) controller and the Model Predictive Control (MPC) controller. For each of these controllers, we will briefly present their theoretical background, the design choices that have been made and the results that have been obtained.
The controllers have been designed and tested in simulation using the Simulink environment, and then implemented on the real system. The results presented in this section are the one obtained from the real system, unless otherwise specified.

6.1 PID Controllers

The Proportional-Integral-Derivative (PID) controller is a simple controller that uses the error signal, its history and its derivative to compute the control signal. It is a widely used controller in industry due to its simplicity and effectiveness in many applications.
The PID controller is defined by the following equation:

$$u(t) = K_p e(t) + K_i \int_0^t e(\tau)dt + K_d \frac{de(t)}{dt} = K_p \left(e(t) + \frac{1}{T_i} \int_0^t e(\tau)dt + T_d \frac{de(t)}{dt} \right) \tag{32}$$

Where K_p, K_i and K_d are the proportional, integral and derivative gains, respectively. T_i and T_d instead are the integral and derivative time constants, respectively.

6.1.1 PID classic

In its simplest form, the PID is a linear controller whose three gains are tuned based on the linearization of the system.

6.1.2 PID with Anti-Windup correction

Bla bla.

6.1.3 Bla bla bla

6.2 LQR Controller

6.3 MPC Controller

7 Conclusions

References

[1] Wikipedia contributors. Scmaglev — Wikipedia, the free encyclopedia. https://en.wikipedia.org/w/index.php?title=SCMaglev&oldid=1243224393, 2024. [Online; accessed 28-September-2024].

A Literature model

In the literature, the model of the MLS system is often further simplified by considering empirical values associated with the inductances and resistances of the coils. In particular, from the `Inteco` manual, the following set of equations is reported:

$$\begin{cases} \dot{z} = v \\ \dot{v} = m^{-1}\left(-F_{em1} + F_{em2} + mg\right) \\ \dot{I}_1 = \frac{1}{f(z)}\left(-I_1 + kiU_1 + ci\right) \\ \dot{I}_2 = \frac{1}{f(h-2r-z)}\left(-I_2 + kiU_2 + ci\right) \end{cases} \tag{33}$$

Where $f(x)$ is an empirical function that takes into account the variation of the inductances due to the presence of the ball in the magnetic field and has the following form:

$$f(z) = \frac{f_{IP1}}{f_{IP2}} e^{\left(-\frac{z}{f_{IP2}}\right)} \tag{34}$$

While F_{em1} and F_{em2} are the electromagnetic forces acting on the ball and have the following form:

$$\begin{cases} F_{em1} & = \frac{F_{emP1}}{F_{emP2}} e^{-\frac{z}{F_{emP2}}} I_1^2 \\ F_{em2} & = \frac{F_{emP1}}{F_{emP2}} e^{-\frac{h-2r-z}{F_{emP2}}} I_2^2 \end{cases} \tag{35}$$

Also from literature, and in particular from the datasheet of the `Inteco` control unit, we can retrieve the following values about the literature model proposed in Equation 33:

Parameter	**Value**	**Units**
F_{emP1}	$1.7521 \cdot 10^{-2}$	H
F_{emP2}	$5.8231 \cdot 10^{-3}$	m
f_{iP1}	$1.4142 \cdot 10^{-4}$	$m \cdot s$
f_{iP2}	$4.5626 \cdot 10^{-3}$	m
c_i	0.0243	A
k_i	2.5165	A

Table 4: Literature parameters